Shahid Bahonar University of Kerman
Agricultural Biotechnology Journal
Iranian Biotechnology Society
Print ISSN: 2228-6705 Online ISSN: 2228-6500

Sequential morphohistological and scanning electron microscopic developmental study of thymus at prenatal stages in Iraqi Awassi sheep fetuses

Zahraa Mazin Mahdi
Department of Veterinary Anatomy, Veterinary College, Qasim Green University, Babylon 51013, Iraq. E-mail: zahraamazin@vet.uoqasim.edu.iq
Jafar Ghazi Abbas Al-Jebori
* Corresponding author. Department of Veterinary Anatomy, Veterinary College, Qasim Green University, Babylon 51013, Iraq. E-mail: jafar@vet.uoqasim.edu.iq

Abstract

Objective

One of the primary lymphoid organs is the thymus, which is of great importance during prenatal and early life. It is responsible for the growth, maturation, and selection of thymocytes and plays a role in the development of T-cell functional competence and central immune tolerance, which is closely related to its specialized histological architecture. This study investigates the prenatal morphological and histological development of the thymus gland in local Awassi sheep with scanning electron microscopy (SEM).

Materials and methods

Thirty thymus specimens were collected from healthy pregnant ewes at different stages of gestation. Fetal age was determined using the fetal crown rump length (CRL) equation and the specimens were classified into three groups: Group 1: 50–55 days, Group 2: 90–100 days, and Group 3: 130–140 days. scanning electron microscopy (SEM) was used to observe the thymic surface at multiple magnifications. Data analysis of histological and morphological parameters was performed using the Statistical Package for the social sciences (SPSS).

Results

In Group 1, thymus was small, underdeveloped organ with soft lobes and thin capsule without connection between cervical and thoracic part. Scanning electron microscopy and histologically revealed an immature surface structure, irregular thymic cells, an unclear connection between the cortex and the medulla, reflecting early thymic differentiation. While in Group 2, the thymus showed an increase in size and improved lobular organization to revealed a more clearly defined cortical-membrane boundary, the growth of tissue bundles extending from the capsule to the viscera, and a higher density of cortical thymus cells. The medullary region also showed reticular epithelial cells, indicating progressive structural maturation. In group 3, thymus was well-developed with prominent lobes separated by connective tissue septa. Histological and Scanning

observations revealed highly organized visceral tissue, a clear cortical-membrane boundary, extensive reticular epithelial cells, and fully formed Hassall's corpuscles within the medulla, demonstrating advanced prenatal microstructural maturation.

Conclusion

These findings highlight the progressive prenatal maturation of the thymus and underscore its pivotal role in immune system development. Deviations from these normal microstructural patterns may indicate pathological or immunological disorders.

Keywords: Awassi sheep, fetuses, prenatal development, SEM, thymus

Paper Type: Research Paper.

Citation: Mahdi Z. M., Al-Jebori J. G. A. (2026). Sequential morphohistological and scanning electron microscopic developmental study of thymus at prenatal stages in Iraqi Awassi sheep fetuses. *Agricultural Biotechnology Journal,* 18(3), 312-332.

Agricultural Biotechnology Journal, 18(3), 312-332. DOI: 10.22103/jab.2026.27058.1877

Received: February 21, 2026. Received in revised form: April 17, 2026.

Accepted: April 18, 2026. Published online: June 30, 2026.

Publisher: Shahid Bahonar University of Kerman & Iranian Biotechnology Society.

Introduction

The thymus is a primary lymphoid organ responsible for the growth, maturation, and selection of thymocytes, contributing to the development of functional T-cell competence and central immune tolerance, which are tightly linked to its specialized histological architecture. It is of paramount importance during the prenatal and early stages of life, providing the microenvironment necessary for thymic cell proliferation, differentiation, and immune regulation. Although the thymus naturally regresses after puberty, its role in shaping immune competence during early developmental stages remains indispensable (Gulla et al*.,* 2023). The thymus is enclosed within a connective tissue capsule and is divided into lobules by septa that extend into the visceral tissue. Each lobe consists of two distinct regions: an outer cortex rich in immature thymic cells and an inner medulla containing fewer lymphocytes, reticular epithelial cells, and Hassall's corpuscles. These structural components support thymocytes maturation and contribute to central immune tolerance through selective cell-cell interactions (Abbas et al., 2019; van Ewijk et al., 2000). Minor differences have been observed between species in the size, shape, and anatomical location of the thymus gland; however, in mammals, it is typically located in the cranial mediastinum and cervical region, maintaining close anatomical relationships with the heart, trachea, and major blood vessels (Dalley & Agur, 2022). Histologically, the cortex is characterized by a high density of thymic cells supported by epithelial networks, while the medulla exhibits a less dense distribution of lymphocytes, prominent epithelial structures, and

concentric Hassall bodies associated with thymic differentiation and immune homeostasis (Rodewald, 2008*)*. Moreover, small ruminants, particularly native breeds, play a crucial role in the livelihoods of a significant portion of the human population in tropical regions from socio-economic perspectives (Molaei Moghbeli et al., 2013; Mohammadabadi & Nanaei, 2021; Saadatabadi et al., 2023; Mohammadabadi et al., 2024). These animals are essential sources of meat, milk, wool, and hides, contributing to food security and rural incomes. Furthermore, they are well-adapted to harsh environmental conditions, making them vital for pastoral and small-scale farming systems (Hajalizadeh et al., 2021). Given their importance, combined efforts that focus on both effective management strategies and genetic improvement are crucial to enhancing animal productivity and ensuring sustainable development (Mohammadipour Saadatabadi et al., 2022; Vahabzadeh et al., 2020; Amirteymoori et al., 2021; Mohammadabadi et al., 2022). Genetic improvement programs, such as selective breeding, molecular marker-assisted selection, and genomic approaches, can significantly boost desirable traits like growth rate, milk yield, and resistance to diseases (Nejad et al., 2024). The economic and biological efficiency of small ruminant production enterprises generally improves by increasing both productivity and reproductive performance in these animals (Zamani et al., 2011; Safaei et al., 2022; Barazandeh et al., 2016; Mohammadinejad, 2016; Shokri et al., 2023). Enhanced reproductive performance can be achieved through improved nutrition, strategic breeding practices, and advanced reproductive technologies such as artificial insemination and embryo transfer (Noori et al., 2017). By integrating these approaches, small ruminant breeders can improve flock productivity, ensure food security, and contribute to the economic well-being of rural populations (Mohammadabadi et al., 2022). Thus, the present study aimed to investigate the prenatal morphohistological and ultrastructural development of the thymus gland in Awassi sheep fetuses using light microscopy and scanning electron and to correlate these changes with fetal age to provide baseline data for normal thymic maturation. This study provides the first detailed SEM-based ultrastructural description of prenatal thymus development in Awassi sheep and these findings contribute original baseline data that may serve as a reference for future developmental, immunological, and pathological studies.

Materials and Methods

Thirty thymus samples were collected from fifty fetuses of pregnant Awassi ewes slaughtered at Karbala and Babylon Province abattoirs in Iraq. The fetuses were selected based on their normal morphological appearance, absence of congenital abnormalities and availability at the desired gestational ages. Only healthy fetuses with intact membranes and no signs of autolysis were included in the study and fetal age was estimated using the crown–rump length (CRL) formula: X=2.1(Y+17), Where X is the age of fetus in days and Y is crown rump length in centimeters (Fisher, 1991; Noakes et al., 2019; Mohassen and Al-Jebori, 2020). Fetuses were categorized into three prenatal groups (ten fetuses for each group): Group I (50–55 days), Group II (90–100 days), and Group III (130–140 days of gestation). Thymus samples were fixed in 10% neutral buffered formalin, dehydrated through a graded ethanol series, cleared in xylene, and embedded in paraffin. Sections were cut at 5–6 μm using a rotary microtome. Staining included

Hematoxylin & Eosin (H&E) for general morphology, Masson's Trichrome for connective tissue, Periodic Acid–Schiff (PAS) for basement membranes and glycoproteins and Tolidine blue for enhance visualization of thymic architecture, thymocytes and reticuloepithelial cells in thymus gland. Small thymus blocks (~1 mm^3) were fixed in 2.5% glutaraldehyde in phosphate buffer (pH 7.4) at 4°C for 24 hours, washed, and post-fixed in 1% osmium tetroxide for 2 hours. Samples were dehydrated in a graded ethanol series (30–100%), dried using critical point drying, mounted on SEM stubs, and sputter-coated with gold–palladium. SEM was used to observe the thymic surface at multiple magnifications. All procedures were performed following ethical standards for the use of animal tissues in research (Niyf and Al-Jebori, 2024; Bancroft et al., 2018). Data analysis of histological and morphological parameters was performed using the Statistical Package for the social sciences (SPSS) version 24. A one-way analysis of variance was performed, and differences were considered significant at $P < 0.05$.

Results and discussion

Observation during first trimester (days 50–60): During early gestation, sheep foetuses exhibited an average body weight of (81±4) gram and a crown-rump length (9±0.69) mm. The thymus was observed as a small, lobulated organ positioned bilaterally in the cranial mediastinum, extending dorsally along the trachea and ventral to the great vessels. The current study is consistent with Ramayyai et al. (2008) in buffalo foetuses, McGeady et al. (2006) in ruminants, Kumar et al. (2015) in goat foetuses and Šinkora & Butler (2009) in pig foetuses. Morphometric measurements of current study showed the thymus cervical and thoracic parts to weigh approximately (0.55±0.072, 0.13 ± 0.04) gram, with a length (12.20±1.9), right arm (8.60±1.14) and thoracic (5.93 ± 0.05) mm and a thickness of left cervical arm (0.96±0.09), right cervical arm (0.80±0.10) and thoracic (3.33 ± 0.04) mm (Tables 1 and 2; Figure 1). Macroscopically, the thymus appeared pale pink and soft in texture. The thoracic part was smaller than cervical, an equilateral triangle, appearance resembles grapes in shape located at the beginning of the branching of the aorta and base of heart (Figure 2). Microscopical analysis revealed that the organ was encapsulated by a thin connective tissue layer (7.89±0.23) μm in thickness (Figures 3 and 4), which extended septa dividing the thymic parenchyma into incomplete lobules. Comparable findings have been reported in goat foetuses (Chaurasia & Menaka, 2024). The lobules consisted of undifferentiated mesenchymal tissue without clear cortical and medullary distinction (Figure 4). Primitive blood vessels detected beneath the capsule, and rudimentary trabecular extensions were observed penetrating into the parenchyma. The findings indicate an early stage of thymic structural development and these findings are consistent with the observations of Chaurasia & Menaka (2024) in goat foetuses, Sarma et al. (2004) in bakarwali goats, Uppal et al. (2007) in buffalo calves, and Chuluunbaatar et al. (2023) in goats and pigs. Scanning electron microscope analysis revealed an immature and loosely organized thymic architecture predominantly composed of few lymphocytes and reticuloepithelial cells. The thymic surface exhibited a three-dimensional, porous framework, forming an interconnected epithelial meshwork and be wrinkles. Reticuloepithelial cells were large, irregular, and stellate, with elongated cytoplasmic processes forming an interdigitating stromal network. Their surfaces were relatively smooth, indicating

early differentiation. Lymphocytes were few, rounded to oval, and variable in size, with wide intercellular spaces. No clear cortical or medullary differentiation was observed at this stage (Figure 5 and 6) and this showed by (Owen & Ritter, 1969; Drenckhahn et al., 1979) who described the early thymus as poorly differentiated, with indistinct corticomedullary separation, a primitive stellate epithelial reticular cell network, and sparse immature thymocytes.

Table 1. Mean (± SEM) values of thickness, width, length and weight of the left and right cervical arms of the thymus gland in sheep fetuses during different prenatal developmental periods

Periods	Left cervical arm thickness (mm)	Right cervical arm thickness (mm)	Left cervical arm width (mm)	Right cervical arm width (mm)	Left cervical arm length (mm)	Right cervical arm length (mm)	Left cervical arm weight (g)	Right cervical arm weight (g)
50–55 days of gestation	0.80±0.10 A	0.96±0.09 A	1.08±0.17 A	0.91±0.08 A	8.60±1.14 A	12.20±1.90 A	0.08±0.01 A	0.13±0.03 A
90–100 days of gestation	1.51±0.04 B	1.80±0.03 B	4.32±0.48 B	4.71±0.46 B	36.00±3.16 B	40.16±1.22 B	0.14±0.05 B	0.25±0.04 B
130–140 days of gestation	4.90±0.09 C	5.11±0.12 C	5.78±0.50 C	8.04±0.40 C	95.52±0.40 C	73.39±2.09 C	0.93±0.03 C	1.14±0.07 C

Means ± standard error of the mean (SEM). Means with different superscript letters (A, B, C) within the same column are significantly different ($P < 0.05$).

Table 2. Morphometric parameters of the thoracic part of the thymus gland in sheep foetuses at different prenatal stages

Gestational age (days)	Body weight (g)	Thoracic weight (g)	Length (mm)	Width (mm)	Thickness (mm)
50–55	81 ± 4^{a}	0.13 ± 0.04^{a}	5.93 ± 0.05^{a}	5.19 ± 0.29^{a}	3.33 ± 0.04^{a}
90–100	486 ± 12^{b}	0.25 ± 0.04^{b}	11.30 ± 0.04^{b}	6.73 ± 0.21^{b}	6.73 ± 0.21^{b}
130–140	3700 ± 150^{c}	2.04 ± 0.38^{c}	20.20 ± 3.70^{c}	16.50 ± 0.5^{c}	8.63 ± 0.04^{c}

Different superscript letters (a, b, c) within the same column indicate significant differences ($P < 0.05$).

The observed interspecies differences in the histological organization of the thymus can be attributed to inherent variations in developmental timing, genetic programming, and fetal endocrine regulation and gestational periods for each breed. Each species follows a distinct thymus differentiation trajectory; therefore, structures such as the capsule, cortical and medullary

regions, lobes, and cellular components may appear clearly defined in some species at a given gestational age while remaining less developed in others.

Figure 1. Photograph of the thymus gland in the first trimester of gestation, showing a pale pink color, composed of cervical and thoracic parts, and located in the neck and thoracic cavity

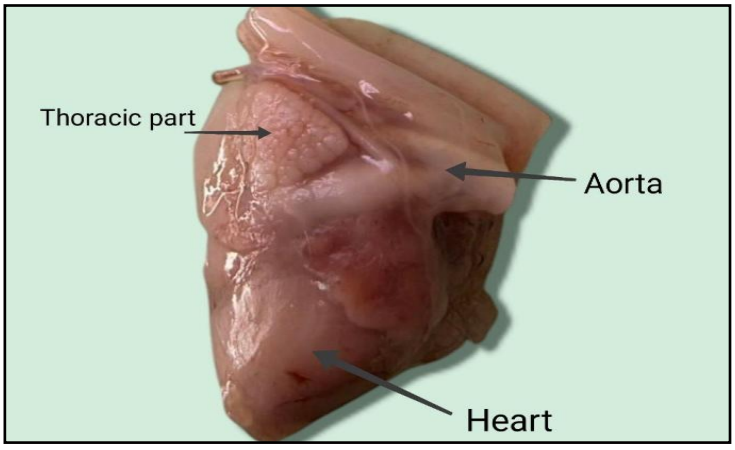

Figure 2. Photograph of the thymus gland in the first trimester of gestation, showing the thoracic part located at the beginning of the aortic arch and at the base of the heart

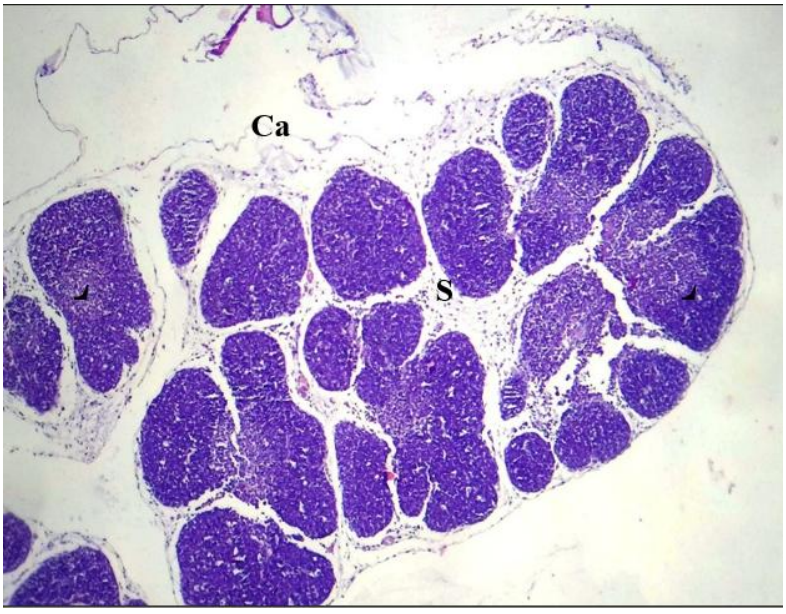

Figure 3. Histological cross-section of the cervical part of the fetal thymus gland during the first trimester of gestation. Ca, capsule; S, septa; L, lobes. (H&E stain, ×4)

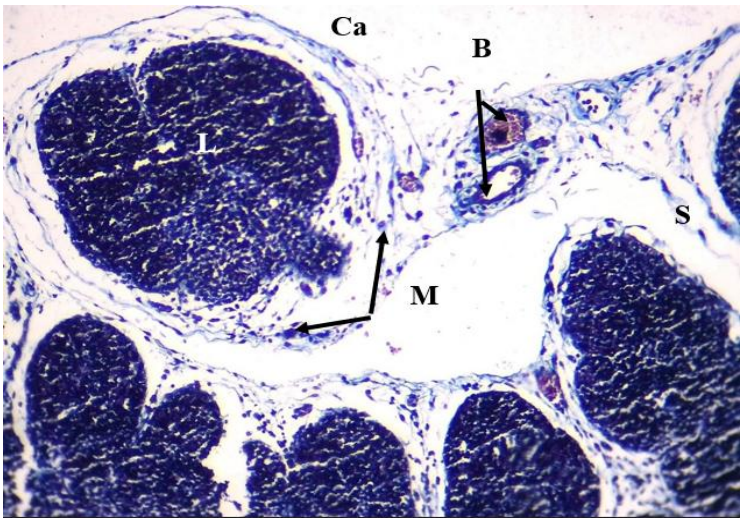

Figure 4. Histological cross-section of the cervical part of the fetal thymus gland during the first trimester of gestation. Ca, capsule; S, septa; L, lobes; B, blood vessels; M, lymphoblasts. (Masson's trichrome stain, ×10)

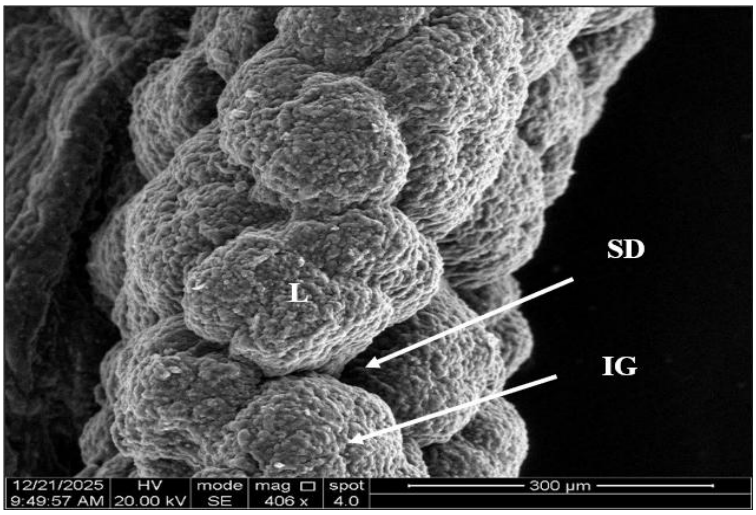

Figure 5. Scanning electron micrograph of the thymus gland during the first trimester of gestation. L, thymic lobule; IG, interlobular groove; SD, septal depression

Observation during second trimester (days 90–100): By mid-gestation, fetal body weight increased to approximately (486± 12) gram, with crown rump length (260±6.53) mm. The thymus exhibited notable growth weight of cervical and thoracic part (1.02±0.12, 0.25 ± 0.04) gram, with a length of cervical, left and right arm (40.16±1.22, 36±3.16) mm, respectively and thoracic part (11.30±0.04) mm and a thickness of cervical, left and right arm (1.80±0.03, 1.51±0.04) mm respectively and thoracic part (6.73±0.21) mm (Tables 1 and 2). Morphologically, the thymus was firmer texture, softness in consistency and exhibits a pinkish-gray in color (Figure 7) as reported earlier by Raghavan (1964) in ox, McGeady et al. (2006) in domestic animals, Berg et al. (1969) in buffalo fetus and Šinkora & Butler (2009) in pig fetus and developed two distinct lobes

connected by a thin isthmus and the anterior end of the thymus was adjacent to cranial thoracic inlet, while the posterior end extended to the pericardial surface (Figure 8).

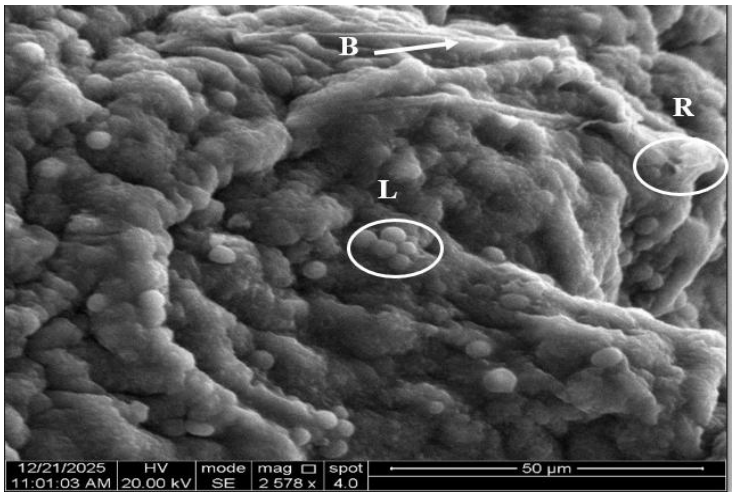

Figure 6. Scanning electron micrograph of the thymus gland during the first trimester of gestation, showing lymphocytes (L), blood vessels (B), and reticuloepithelial cells (R). The thymic surface exhibits a three-dimensional porous framework forming an interconnected epithelial meshwork with surface wrinkles.

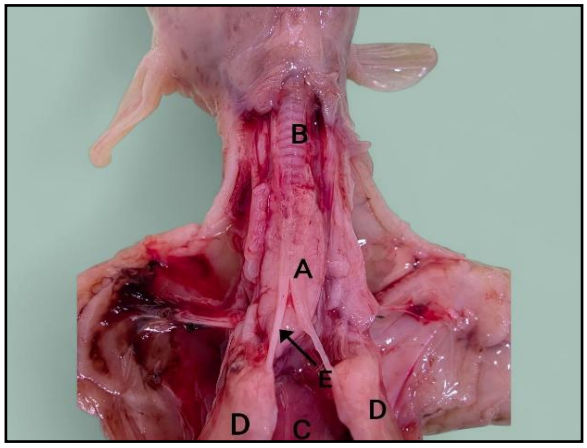

Figure 7. Photograph of the fetus during the second trimester of gestation, showing the body (A), tracheal rings (B), heart (C), and left and right lobes of the lungs (D)

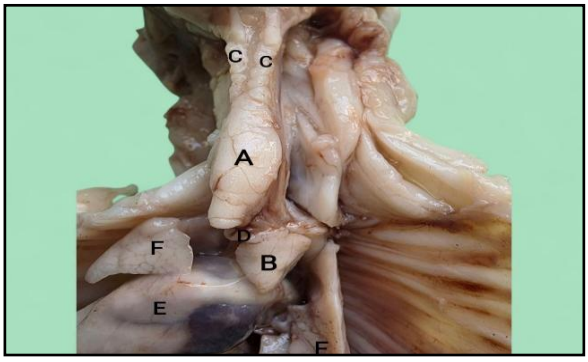

Figure 8. Photograph of the fetus during the second trimester of gestation, showing the body (A), thoracic part of the thymus gland (B), left and right forelimbs (C), isthmus of the thymus gland (D), heart (E), and left and right lobes of the lungs (F)

Histologically, the thymus exhibited advanced structural organization characterized by a fully lobulated architecture. The capsule and interlobular septa consisted primarily of collagen fibers with sparse elastic and reticular fibers. Septal trabeculae penetrated into the parenchyma, subdividing it into multiple compartments, with the parenchyma subdivided into outer cortex and central medulla. (Figure 9). The thymocytes were densely packed in the cortical region, while medullary regions contained scattered epithelial reticular cells. Small blood vessels were evident throughout the parenchyma, reflecting the early vascularization essential for lymphoid differentiation (Figure 10). These results corresponded with observations in buffalo calves described by Ramayyai et al. (2008) and Bhagyalakshmi et al. (2023) in sheep and consistent with earlier findings in goat fetuses reported by Chaurasia & Menaka (2024) and Mainde et al. (2018). During the mid-prenatal period (90–100 days), the thymus showed a significant increase ($P<0.05$) in all biometrical parameters compared to the early stage, with marked growth of both thoracic and cervical parts, indicating active organogenesis and lobulation. Histologically, clear corticomedullary differentiation, well-formed lobules with interlobular septa, increased cortical thickness, and the appearance of small Hassall's corpuscles were observed, reflecting enhanced thymocytes proliferation and progressive functional maturation.

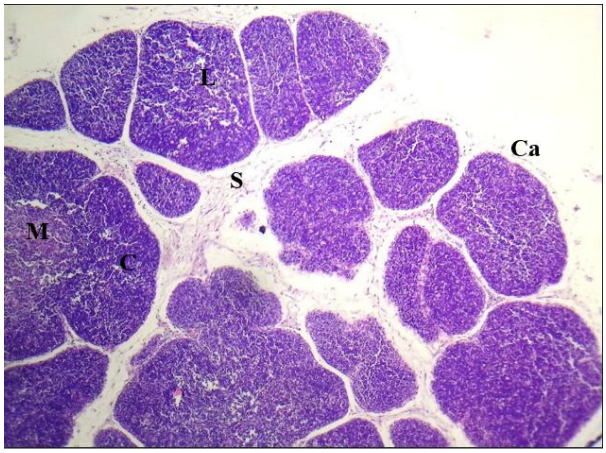

Figure 9. Histological cross-section of the fetal thymus gland during the second trimester of gestation. Ca, capsule; S, septa; L, lobes; C, cortex; M, medulla (H&E stain, ×4)

Scanning electron microscope imaging highlighted the fine structural organization of thymic lobules, revealed partial lobulation, with the appearance of shallow grooves and septa-like depressions separating developing lobules (Figure 11). Cellular elements appeared more uniformly distributed, indicating progressive differentiation of thymocytes and maturation of the reticuloepithelial cell network. Intercellular spaces were more evident, suggesting increased cellular migration and stromal organization (Figure 12). These features reflect the establishment of the thymic microenvironment required for lymphoid development.

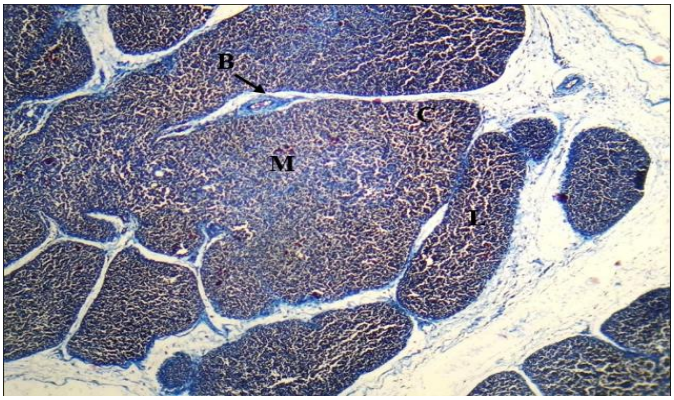

Figure 10. Histological cross-section of the fetal thymus gland during the second trimester of gestation, showing lobes (L), blood vessels (B), cortex (C), and medulla (M). Increased collagen, elastic, and reticular fibers are observed within the capsule, interlobular septa, and trabeculae, appearing blue with Masson's trichrome stain. (Masson's trichrome stain, ×4)

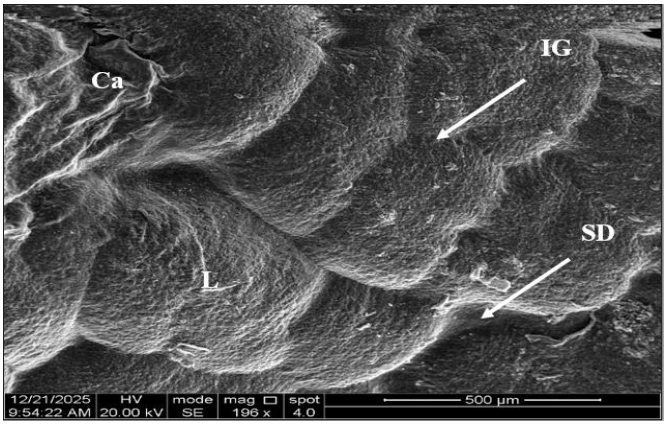

Figure 11. Scanning electron micrograph of the thymus gland during the second trimester of gestation, showing lobes (L), capsule (Ca), interlobular grooves (IG), and septal depressions (SD). The surface exhibits shallow grooves and septa-like depressions separating the developing lobules

During the mid-prenatal period (90–100 days), the thymus exhibited a statistically significant increase ($P<0.05$) in all biometric parameters compared to the early stage. The thoracic part showed marked enlargement in length, width, and thickness, while the cervical part demonstrated increased weight and length with evident cranial and caudal expansion, reflecting accelerated tissue differentiation and lobulation. This morphological progression corresponds with enhanced thymocyte proliferation and initiation of T-cell receptor rearrangement, alongside a more distinct corticomedullary organization indicative of early immune selection processes. Histologically, the thymus displayed well-defined lobules separated by prominent interlobular septa, with clear cortical and medullary differentiation. Morphometric analysis revealed increased lobular diameter and cortical thickness, as well as the appearance of small Hassall's corpuscles within the medulla, suggesting progressive epithelial maturation and functional development.

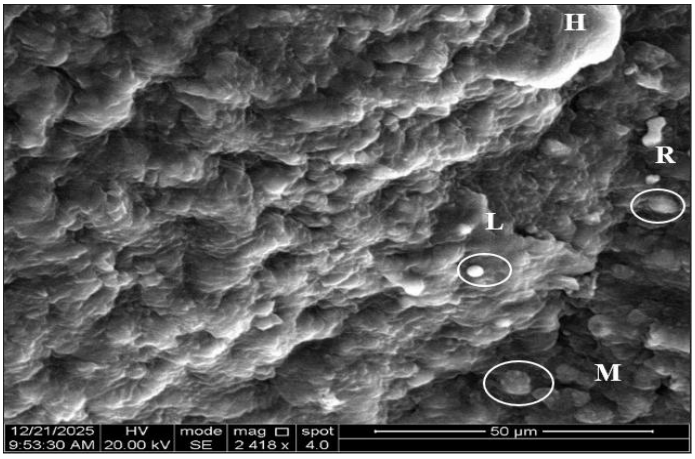

Figure 12. Scanning electron micrograph of the thymus gland at 90 days of gestation, showing lymphocytes (L), reticuloepithelial cells (R), Hassall's corpuscles (H), and macrophages (M)

Observation during third trimester (days 130–140): During the later stages of gestation, the average body weight of the sheep foetuses was (3700± 150) gram, and their crown rump length was (400±10.09) mm. The thymus grew significantly compared to earlier stages, weighing approximately (3.57±0.122, 2.04 ± 0.38) gram in cervical and thoracic part respectively, measuring (73.39±2.09, 95.52±0.48) mm in left and right arms (20.20 ± 3.70) mm in thoracic part in length, and (5.11±0.12, 4.90±0.095) mm in left and right arms (8.63±0.04) mm in thoracic part in thickness (Tables 1 and 2). Morphologically, the thymus was well-lobulated elongated mass and widely distributed, located on either side of the anterior mediastinum, and extended along the trachea and above the pericardial region. The two lobes were connected by a thin isthmus, whitish-gray with a firm consistency and the organ's surface was smooth. (Figure 13) These findings are consistent with previous reports across various species according to Chaurasia (2022) in the Surti goat foetuses. Its anterior end was adjacent to the thoracic inlet, was quadrilateral, flattened in shape, pale pink to light beige parenchymal tissue comprised of several lobules, and in situ, the thoracic thymus occupies the superior and anterior mediastinum, extending inferiorly toward the pericardium. while its posterior end extended towards the pericardium and major blood vessels (Figure 14). These findings corroborate the descriptions by Raghavan (1964) in ox, Schummer et al. (1981) in bovines, and Ramayyai et al. (2008) in buffalo foetuses. Histological examination approved high number of lobules and irregular in shape surrounded by thin connective tissue capsule, thymic lobular organization and cortical-membrane differentiation were more pronounced than in the first two trimesters of pregnancy, reflecting increased, the thymic cortex is well-developed and densely populated with immature thymic cells. The medulla becomes more differentiated, containing more mature thymic cells and characteristic Hassall's bodies, the reticular fibres became more consolidated, appearing thick and continuous in stroma and parenchyma. (Figure 15).

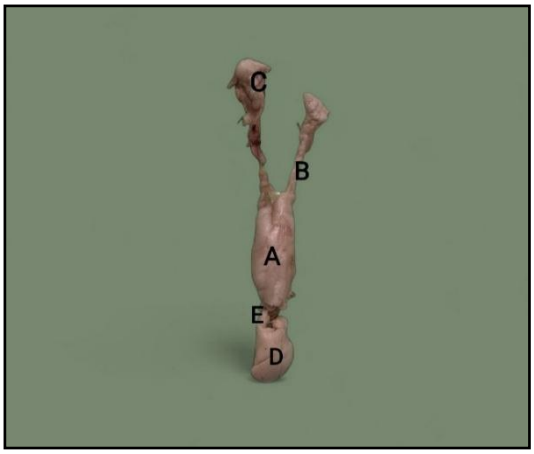

Figure 13. Photograph of the fetus during the third trimester of gestation, showing the body (A), left arm (B), right arm (C), thoracic part of the thymus gland (D), and thymic isthmus (E)

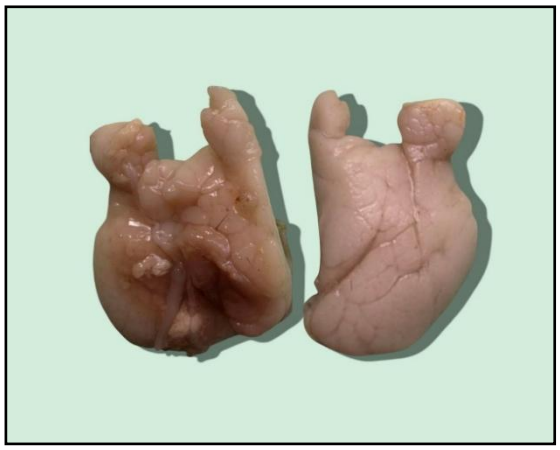

Figure 14. Photograph of the fetus during the third trimester of gestation, showing the parietal and visceral surfaces of the thoracic part of the thymus gland

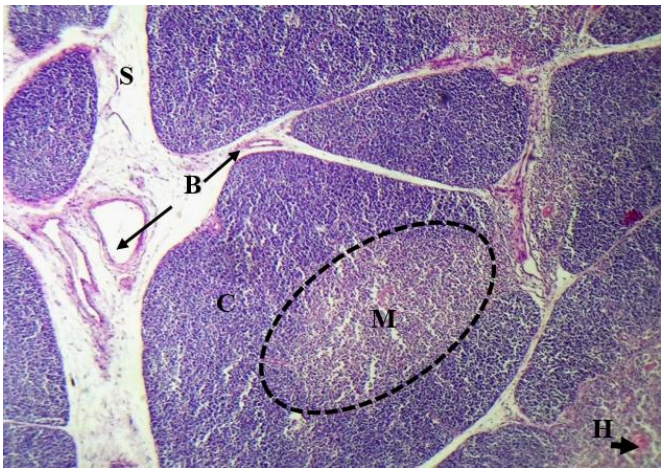

Figure 15. Histological cross-section of the fetal thymus gland during the third trimester of gestation. H, Hassall's corpuscles; C, cortex; M, medulla; S, septa; B, blood vessels. (H&E stain, ×4)

Hassall's corpuscles showed an increase in both number and size, with more distinctly defined concentric lamellae. Two main types were recognized: uni-lamellar corpuscles and multilamellar corpuscles (Figure 16). These findings are consistent with those of Berg et al. (1969) in buffalo foetuses and Chaurasia & Menaka (2024) in goat foetuses.

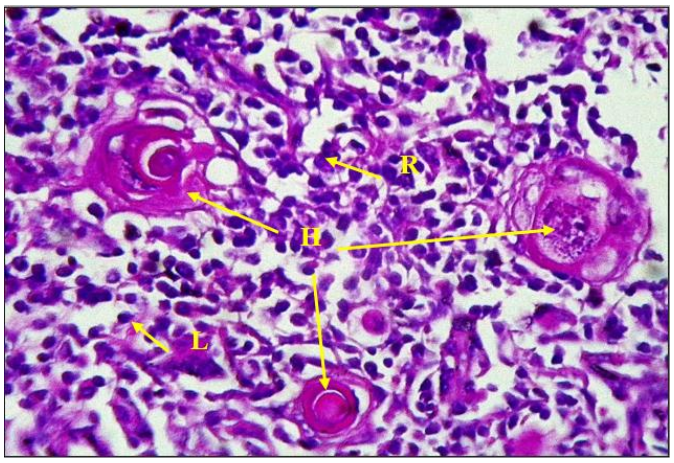

Figure 16. Histological cross-section of the fetal thymus gland during the third trimester of gestation. L, thymocytes; R, reticuloepithelial cells; H, Hassall's corpuscles, which are classified into two main types: unilamellar and multilamellar corpuscles. (H&E stain, ×40)

Scanning electron microscopy (SEM) revealed that the thymic gland exhibited a well-developed and distinctly lobulated surface architecture. Clearly defined lobular boundaries were observed, separated by prominent grooves and well-formed septal depressions. The thymic surface appeared more organized and less irregular, displaying broader surface folds and relatively smooth contours when compared with earlier developmental stages (Figure 17).

These findings are consistent with those of van Ewijk (1984). The cellular arrangement suggested advanced thymocytes maturation, supported by a fully developed reticuloepithelial framework. Increased surface complexity and expanded intercellular spaces indicate functional readiness of the thymus prior to birth (Figure 18). During the late prenatal stage (130–140 days), the thymus attained maximal biometrical values ($P<0.05$), with significant enlargement of both cervical and thoracic regions, indicating advanced organ maturation. Histologically, it exhibited well-developed lobulation with prominent interlobular septa, a thick, densely cellular cortex, and an extensive, highly organized medulla. Morphometric parameters revealed peak lobular diameter and cortical thickness, along with a marked expansion of the medullary area. Numerous Hassall's corpuscles of varying sizes and increased vascularization were evident, reflecting intensified thymic activity and advanced functional maturation in preparation for postnatal immune competence. During the late prenatal period (130–140 days), the thymus attained its highest biometric values, with all morphological parameters showing a significant increase ($P<0.05$) compared to the mid stage. Both cervical and thoracic parts exhibited maximal growth in weight, length, width, and thickness; the thoracic thymus became broader and more triangular, while the cervical segment showed marked expansion, reflecting advanced maturation. Functionally, this stage corresponds to peak intrauterine thymic activity, characterized by maximal T-cell

maturation, establishment of central tolerance, and enhanced export of naïve T lymphocytes into circulation.

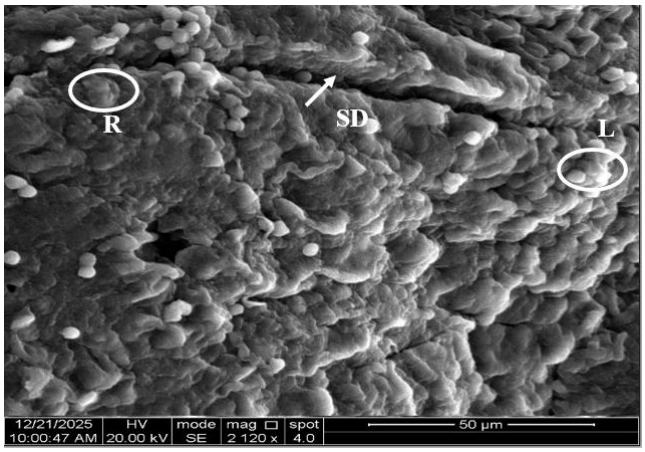

Figure 17. Scanning electron micrograph of the thymus gland during the third trimester of gestation, showing lymphocytes (L), reticuloepithelial cells (R), and septal depressions (SD). The thymic surface exhibits a well-developed, distinctly lobulated architecture with clearly defined lobular boundaries

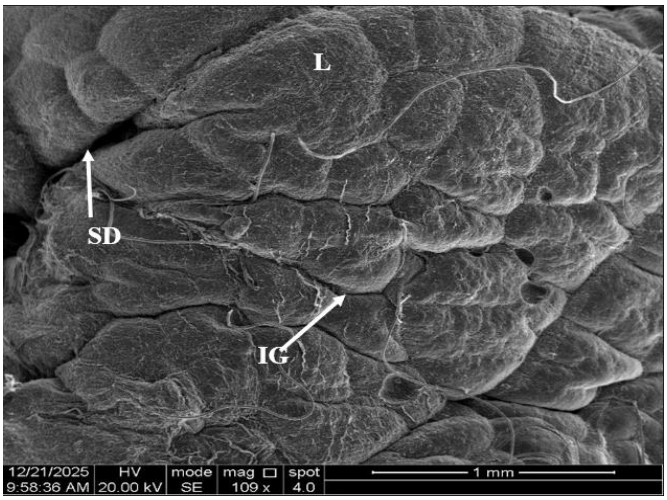

Figure 18. Scanning electron micrograph of the thymus gland during the third trimester of gestation, showing lobes (L), interlobular grooves (IG), and septal depressions (SD)

Histologically, the gland displayed well-developed lobes with a thick, densely cellular cortex and an extensive, highly organized medulla accompanied by more evident intramedullary perfusion, indicating heightened functional activity. These findings are consistent with previous reports describing progressive thymic growth toward late gestation in species such as goats and pigs (Šinkora & Butler, 2009; Chaurasia, 2022).

Conclusions: This study concluded that the thymus gland in sheep undergoes distinct age-dependent morphological and histological changes during prenatal development. Morphologically, the thymus exhibited a gradual increase in size and lobes with advancing gestational age, accompanied by progressive maturation of the connective tissue capsule and trabeculae. Histologically, cortical-medullary differentiation became evident in late gestation,

with the cortex exhibiting high cellular density and the medulla lower cellular density. Scanning electron microscopy revealed an increase in cellular density, surface complexity, and thymic cell organization with advancing age, along with a more prominent presence of macrophages involved in the removal of dead cells.

Novelty statement: Present report and finding can advanced several aspects of the Thymus development and offer several markers to be considered during effective assess of animal health and production potential.

Author's contribution

Zahraa Mazin Mahdi and Jafar Ghazi Abbas confirm contribution to the paper equally.

Data availability statement

The datasets used and/or analyzed during the current study are available from the corresponding author on reasonable request.

Acknowledgement

The authors gratefully acknowledge the support of al- Qasim green university and thank all colleagues and staff who contributed to the success of this study.

Ethical considerations

The experimental procedures were approved by the Institutional Animal Ethics Committee and conducted at the Veterinary Medicine College, Al-Qassim Green University, Iraq. Ethical regulation of this work was assigned by the university research committee and adhered to the guidelines of the American Veterinary Medical.

Funding

This research is supported by the Department of Veterinary Anatomy, Veterinary College, Qasim Green University, Babylon, Iraq.

Conflict of interest

The authors have no conflict to declare.

References

Abbas, A. K., Lichtman, A. H., & Pillai, S. (2019). *Basic immunology: Functions and disorders of the immune system* (6th ed.). Elsevier.

Amirteymoori, E., Khezri, A., Dayani, O., Mohammadabadi, M., Khorasani, S., Mousaie, A., & Kazemi-Bonchenari, M. (2021). Effects of linseed processing method (ground versus extruded) and dietary crude protein content on performance, digestibility, ruminal fermentation pattern, and rumen protozoa population in growing lambs. *Italian Journal of Animal Science, 20*(1), 1506–1517. https://doi.org/10.1080/1828051X.2021.1984324

Bancroft, J. D., Suvarna, K. S., & Layton, C. (2018). *Bancroft's theory and practice of histological techniques* (8th ed.). Elsevier Health Sciences. https://doi.org/10.1016/C2015-0-00143-5

Barazandeh, A., Mohammadabadi, M. R., Ghaderi-Zefrehei, M., & Nezamabadipour, H. (2016). Predicting CpG islands and their relationship with genomic features in cattle by hidden Markov model algorithm. *Iranian Journal of Applied Animal Science, 6*(3), 571–579.

Berg, R., Taher, E.-S., & Moustafa, M. S. E. D. M. (1969). Comparative studies on the prenatal growth of the brain, thymus, stomach and oesophagus in the camel (*Camelus dromedarius*) and Egyptian water buffalo (*Bos/Bubalus bubalis* L.). *Zentralblatt für Veterinärmedizin Reihe A, 16*, 659–663. https://doi.org/10.1111/j.1439-0442.1969.tb00767.x

Bhagyalakshmi, J., Balasundaram, K., & Raju, N. K. B. (2023). Histological observations on prenatal development of thymus in sheep. *The Haryana Veterinarian, 62*(SI-2), 96–99. https://www.luvas.edu.in/haryana-veterinarian/archive-2023.php?AM19

Chaurasia, S. (2022). Gross and morphometrical studies on the thymus of prenatal Surti goat (*Capra hircus*). *Indian Journal of Veterinary Anatomy, 33*(2), 85–88. https://epubs.icar.org.in/index.php/IJVA/article/view/120488

Chaurasia, S., & Menaka, R. (2024). Histogenesis of thymus in prenatal Surti goats. *Indian Journal of Veterinary Anatomy, 36*(1), 60–64. https://epubs.icar.org.in/index.php/IJVA/article/view/162039

Chuluunbaatar, T., Ichii, O., Masum, M. A., Namba, T., & Kon, Y. (2023). Morphological characteristics of genital organ-associated lymphoid tissue in the vaginal vestibule of goats and pigs. *Veterinary Sciences, 10*(1), Article 51. https://doi.org/10.3390/vetsci10010051

Dalley, A. F., & Agur, A. M. R. (2022). *Moore's clinically oriented anatomy* (9th ed.). Wolters Kluwer.

Drenckhahn, D., von Gaudecker, B., Müller-Hermelink, H. K., Unsicker, K., & Gröschel-Stewart, U. (1979). Myosin and actin containing cells in the human postnatal thymus: Ultrastructural and immunohistochemical findings in normal thymus and in myasthenia gravis. *Virchows Archiv B Cell Pathology Including Molecular Pathology, 32*(1), 33–45. https://doi.org/10.1007/BF02889011

Fisher, D. A. (1991). Thyroid system ontogeny in the sheep: A model for precocial mammalian species. *Advances in Experimental Medicine and Biology, 299*, 11–26. https://doi.org/10.1007/978-1-4684-5973-9_2

Gulla, S., Reddy, M. C., Reddy, V. C., Chitta, S., Bhanoori, M., & Lomada, D. (2023). Role of thymus in health and disease. *International Reviews of Immunology, 42*(5), 347–363. https://doi.org/10.1080/08830185.2022.2064461

Hajalizadeh, Z., Dayani, O., Khezri, A., Tahmasbi, R., Mohammadabadi, M., Solodka, T., Kalashnyk, O., Afanasenko, V., & Babenko, O. (2021). Expression of calpastatin gene in Kermani sheep using real-time PCR. *Journal of Livestock Science and Technology, 9*(2), 51–57. https://doi.org/10.22103/jlst.2021.18165.1381

Kumar, V., Singh, S. P., Farooqui, M. M., Kumar, P., Prakash, A., & Archana. (2015). Gross and biometrical studies of placentome in goat (*Capra hircus*) during different stages of pregnancy. *Journal of Animal Research, 5*(2), 251–255. https://doi.org/10.5958/2277-940X.2015.00040.0 (Note: Semantic Scholar link retained if no DOI; adjust if needed.)

Mainde, U. P., Nandeshwar, N. C., Dalvi, R. S., Banubakode, S. B., Salankar, A. M., Sathapathy, S., & Rana, J. (2017). Histogenesis of thymus in different prenatal age groups of goat foetus. *Indian Journal of Veterinary Anatomy, 29*(1), 5–6. https://epubs.icar.org.in/index.php/IJVA/article/view/83058

McGeady, T. A., Quinn, P. J., FitzPatrick, E. S., & Ryan, M. T. (2006). Forms of implantation and placentation. In T. A. McGeady, P. J. Quinn, E. S. FitzPatrick, & M. T. Ryan, *Veterinary embryology* (pp. 87–104). Blackwell Publishing.

Mohammadabadi, M. R., Shaban Jorjandy, D., Arabpoor Raghabadi, Z., Abareghi, F., Sasan, H. A., & Bordbar, F. (2022). The role of fennel on DLK1 gene expression in sheep heart tissue. *Agricultural Biotechnology Journal, 14*(2), 155–170. https://doi.org/10.22103/jab.2022.19402.1399

Mohammadabadi, M. R. (2016). Inter-simple sequence repeat loci associations with predicted breeding values of body weight in Kermani sheep. *Genetics in the Third Millennium, 14*(4), 4386–4393.

Mohammadabadi, M., & Nanaei, H. A. (2021). Leptin gene expression in Raini Cashmere goat using real-time PCR. *Agricultural Biotechnology Journal*. https://doi.org/10.22103/JAB.2021.17334.1305

Mohammadabadi, M., Babenko, O., Borshch, O. O., Kalashnyk, O., Ievstafiieva, Y., & Buchkovska, V. (2024). Measurement of the relative expression pattern of the UCP2 gene in different tissues of the Raini Cashmere goat. *Agricultural Biotechnology Journal, 16*(3), 317–332. https://doi.org/10.22103/jab.2024.24337.1627

Mohammadabadi, M., Kheyrodin, H., Latifi, A., & Babenko, O. I. (2022). mRNA expression profile of DNAH1 gene in testis tissue of Raini Cashmere goat. *Agricultural Biotechnology Journal*. https://doi.org/10.22103/jab.2022.20199.1428

Mohammadinejad, F., Mohammadabadi, M., Roudbari, Z., & Sadkowski, T. (2022). Identification of key genes and biological pathways associated with skeletal muscle maturation and hypertrophy in *Bos taurus*, *Ovis aries*, and *Sus scrofa*. *Animals, 12*(24), Article 3471. https://doi.org/10.3390/ani12243471

Mohammadipour Saadatabadi, L. M., Mohammadabadi, M., Nanaei, H. A., Ghanatsaman, Z. A., Stavetska, R. V., Kalashnyk, O., Kochuk-Yashchenko, O. A., & Kucher, D. M. (2023). Unraveling candidate genes related to heat tolerance and immune response traits in some native sheep using whole genome sequencing data. *Small Ruminant Research, 225*, Article 107018. https://doi.org/10.1016/j.smallrumres.2023.107018

Mohassen, F. W., & Al-Jebori, J. G. A. (2020). Ontogenesis of thyroid gland in Awasi sheep foetuses: Prenatal study. *Plant Archives, 20*(Suppl. 1), 1096–1100. http://www.plantarchives.org/SPECIAL%20ISSUE%2020-1/1096-1100%20(64).pdf

Molaei Moghbeli, S., Barazandeh, A., Vatankhah, M., & Mohammadabadi, M. (2013). Genetics and non-genetics parameters of body weight for post-weaning traits in Raini Cashmere goats. *Tropical Animal Health and Production, 45*, 1519–1524. https://doi.org/10.1007/s11250-013-0393-4

Nejad, F. M., Mohammadabadi, M., Roudbari, Z., et al. (2024). Network visualization of genes involved in skeletal muscle myogenesis in livestock animals. *BMC Genomics, 25*, Article 294. https://doi.org/10.1186/s12864-024-10196-3

Niyf, A. M., & Al-Jebori, J. G. A. (2024). Ontogenesis of rectum in local Awassi sheep fetuses (*Ovis aries*) during prenatal periods. *Journal of Animal Health and Production, 12*(s1), 45–54. https://doi.org/10.17582/journal.jahp/2024/12.s1.45.54

Noakes, D. E., Parkinson, T. J., & England, G. C. W. (Eds.). (2019). *Veterinary reproduction and obstetrics* (10th ed.). Saunders Ltd. https://doi.org/10.1016/C2014-0-04782-X

Noori, A. N., Behzadi, M. R. B., & Mohammadabadi, M. R. (2017). Expression pattern of Rheb gene in Jabal Barez Red goat. *The Indian Journal of Animal Sciences, 87*(11), 1375–1378. https://doi.org/10.56093/ijans.v87i11.75890

Owen, J. J., & Ritter, M. A. (1969). Tissue interaction in the development of thymus lymphocytes. *Journal of Experimental Medicine, 129*(2), 431–442. https://doi.org/10.1084/jem.129.2.431

Raghavan, D. (Ed.). (1964). *Anatomy of the ox: With comparative notes on the horse, dog and fowl*. Indian Council of Agricultural Research.

Ramayyai, P. J., Singh, O., & Roy, K. S. (2008). Gross anatomical studies on the thymus of pre- and post-natal buffalo (*Bubalus bubalis*). *The Indian Journal of Animal Sciences, 78*(5), 461–464. https://epubs.icar.org.in/index.php/IJAnS/article/view/4714

Rodewald, H. R. (2008). Thymus organogenesis. *Annual Review of Immunology, 26*, 355–388. https://doi.org/10.1146/annurev.immunol.26.021607.090408

Saadatabadi, L. M., Mohammadabadi, M., Ghanatsaman, Z. A., Babenko, O., Stavetska, R. V., Kalashnik, O. M., Afanasenko, V., Kochuk-Yashchenko, O. A., Kucher, D. M., & Nanaei, H. A. (2023). Data of whole-genome sequencing of Karakul, Zel, and Kermani sheep breeds. *BMC Research Notes, 16*(1), Article 353. https://doi.org/10.1186/s13104-023-06630-6

Safaei, S. M. H., Dadpasand, M., Mohammadabadi, M., Atashi, H., Stavetska, R., Klopenko, N., & Kalashnyk, O. (2022). An Origanum majorana leaf diet influences myogenin gene expression, performance, and carcass characteristics in lambs. *Animals, 13*(1), Article 14. https://doi.org/10.3390/ani13010014

Sarma, K., Kalita, A., Suri, S., & Zama, M. M. S. (2004). Gross anatomical observations on superficial lymph nodes of Bakarwali goat (*Capra hircus*). *The Indian Journal of Animal Sciences, 74*(7), 750–751. https://epubs.icar.org.in/index.php/IJAnS/article/view/39039

Schummer, A., Wilkens, H., Vollmerhaus, B., & Habermehl, K.-H. (1981). *The circulatory system, the skin, and the cutaneous organs of the domestic mammals*. Springer. https://doi.org/10.1007/978-1-4899-7102-9

Shokri, S., Khezri, A., Mohammadabadi, M., & Kheyrodin, H. (2023). The expression of MYH7 gene in femur, humeral muscle, and back muscle tissues of fattening lambs of the Kermani breed. *Agricultural Biotechnology Journal, 15*(2), 217–236. https://doi.org/10.22103/jab.2023.21524.1486

Šinkora, M., & Butler, J. E. (2009). The ontogeny of the porcine immune system. *Developmental & Comparative Immunology, 33*(3), 273–283. https://doi.org/10.1016/j.dci.2008.07.011

Uppal, V., Bansal, N., & Roy, K. S. (2007). Histoenzymic studies on the thymus of neonatal buffalo calves. *The Indian Journal of Animal Sciences, 77*(8), 723–726. https://epubs.icar.org.in/index.php/IJAnS/article/view/10382

Vahabzadeh, M., Chamani, M., Dayani, O., & Sadeghi, A. A. (2020). Effect of Origanum majorana leaf (sweet marjoram) feeding on lamb's growth, carcass characteristics, and blood biochemical parameters. *Small Ruminant Research, 192*, Article 106233. https://doi.org/10.1016/j.smallrumres.2020.106233

van Ewijk, W., Holländer, G., Terhorst, C., & Wang, B. (2000). Stepwise development of thymic microenvironments in vivo is regulated by thymocyte subsets. *Development, 127*(8), 1583–1591. https://doi.org/10.1242/dev.127.8.1583

van Ewijk, W. (1984). Immunohistology of lymphoid and non-lymphoid cells in the thymus in relation to T lymphocyte differentiation. *American Journal of Anatomy, 170*(3), 311–330. https://doi.org/10.1002/aja.1001700307

Zamani, P., Akhondi, M., Mohammadabadi, M. R., Saki, A. A., Ershadi, A., Banabazi, M. H., & Abdolmohammadi, A. R. (2011). Genetic variation of Mehraban sheep using two inter simple sequence repeat (ISSR) markers. *African Journal of Biotechnology, 10*(10), 1812–1817. https://www.ajol.info/index.php/ajb/article/view/93089

مجله بیوتکنولوژی کشاورزی
شاپا چاپی: ۶۷۰۵-۲۲۲۸ شاپا الکترونیکی: ۶۵۰۰-۲۲۲۸
دانشگاه شهید باهنر کرمان
انجمن بیوتکنولوژی ایران

مطالعه توالی تکامل مورفوهیستولوژیک و میکروسکوپ الکترونی روبشی تیموس در مراحل پیش از تولد در جنین‌های گوسفند آواسی عراقی

زهراء مازن مهدی

گروه آناتومی دامپزشکی، دانشکده دامپزشکی، دانشگاه القاسم سبز، بابل ۵۱۰۱۳، عراق. ایمیل: zahraamazin@vet.uoqasim.edu.iq

جعفر غازی عباس الجبوری

* نویسنده مسئول. گروه آناتومی دامپزشکی، دانشکده دامپزشکی، دانشگاه القاسم سبز، بابل ۵۱۰۱۳، عراق. ایمیل: jafar@vet.uoqasim.edu.iq

تاریخ دریافت: ۱۴۰۴/۱۲/۰۲ تاریخ دریافت فایل اصلاح شده نهایی: ۱۴۰۵/۰۱/۲۸ تاریخ پذیرش: ۱۴۰۵/۰۱/۲۹

چکیده

هدف: تیموس یکی از اندام‌های لنفاوی اولیه است که در دوران جنینی و اوایل زندگی اهمیت زیادی دارد. این اندام مسئول رشد، تمایز و انتخاب تیموسیت‌ها بوده و در ایجاد توانایی عملکردی سلول‌های T و تحمل ایمنی مرکزی نقش دارد؛ عملکردی که ارتباط نزدیکی با ساختار بافت‌شناسی تخصص‌یافته آن دارد. هدف این مطالعه بررسی تکامل مورفولوژیک و بافت‌شناسی غده تیموس در دوران پیش از تولد در گوسفندان بومی آواسی با استفاده از میکروسکوپ الکترونی روبشی (SEM) بود.

مواد و روش‌ها: تعداد ۳۰ نمونه تیموس از میش‌های آبستن سالم در مراحل مختلف آبستنی جمع‌آوری شد. سن جنین‌ها با استفاده از طول تاجی–نشستگاهی (CRL) تعیین گردید و نمونه‌ها به سه گروه تقسیم شدند: گروه اول (۵۰–۵۵ روز)، گروه دوم (۹۰–۱۰۰ روز) و گروه سوم (۱۳۰–۱۴۰ روز). برای بررسی سطح تیموس در بزرگنمایی‌های مختلف از میکروسکوپ الکترونی روبشی (SEM) استفاده شد. تحلیل داده‌های مورفولوژیک و بافت‌شناسی با نرم‌افزار SPSS انجام گرفت.

نتایج: در گروه اول، تیموس اندامی کوچک و نابالغ با لوب‌های نرم و کپسول نازک بود و ارتباطی بین بخش‌های گردنی و سینه‌ای مشاهده نشد. بررسی‌های SEM و بافت‌شناسی ساختار سطحی نابالغ، سلول‌های تیموسی نامنظم و تمایز نامشخص بین قشر و مدولا را نشان داد که بیانگر مراحل اولیه تمایز تیموس است. در گروه دوم، افزایش اندازه تیموس و بهبود سازمان‌یافتگی لوبولی مشاهده شد. مرز قشر و مدولا واضح‌تر گردید، رشته‌های بافتی از کپسول به داخل گسترش یافتند و تراکم سلول‌های قشری افزایش

پیدا کرد. همچنین حضور سلول‌های اپی‌تلیالی رتیکولار در ناحیه مدولا نشان‌دهنده بلوغ تدریجی ساختاری بود. در گروه سوم، تیموس به‌طور کامل رشد یافته و دارای لوب‌های مشخص جداشده توسط سپتاهای بافت همبند بود. بررسی‌های بافت‌شناسی و SEM ساختار بسیار سازمان‌یافته، مرز مشخص قشر و مدولا، گسترش وسیع سلول‌های اپی‌تلیالی رتیکولار و تشکیل کامل اجسام هاسال در مدولا را نشان داد که بیانگر بلوغ پیشرفته ریزساختاری در دوران جنینی است.

نتیجه‌گیری: یافته‌های این مطالعه روند تدریجی بلوغ تیموس در دوران پیش از تولد را نشان می‌دهد و نقش حیاتی آن در تکامل سیستم ایمنی را برجسته می‌سازد. هرگونه انحراف از این الگوهای طبیعی ریزساختاری می‌تواند نشان‌دهنده اختلالات پاتولوژیک یا ایمنی باشد.

کلمات کلیدی: تکامل پیش‌زادی، تیموس، جنین، گوسفند آواسی، میکروسکوپ الکترونی روبشی (SEM)

نوع مقاله: پژوهشی

استناد: زهراء مازن مهدی، جعفر غازی عباس الجبوری (۱۴۰۵) مطالعه توالی تکامل مورفوهیستولوژیک و میکروسکوپ الکترونی روبشی تیموس در مراحل پیش از تولد در جنین‌های گوسفند آواسی عراقی. *مجله بیوتکنولوژی کشاورزی*، ۱۸(۳)، ۳۱۲-۳۳۲.

Publisher: Shahid Bahonar University of Kerman & Iranian Biotechnology Society.